Fatigue life estimate in metallic chains links of mooring system

Lucas O. Barros[1], Leonel L. D. Morales[2], Lucival Malcher[1]

[1]*Dept. of Mechanical Engineering, University of Brasilia*
Asa Norte, 70910-900, Brasilia/ Federal District, Brazil
lucasbarros1211@gmail.com, malcher@unb.br
[2]*Austral University of Chile, Faculty of Engineering Sciences, Institute of Design and Industrial Methods,*
General Lagos 2086, Miraflores Campus, Valdivia, Chile
leonel.delgado@uach.cl

Abstract. This contribution proposes the application of the Finite Element Method (FEM) for the study and analysis of chain links of the Floating Production Storage and Offloading (FPSO) ship anchoring system, regarding the level of stress at the hotspots. Besides that, cyclical flexion occurred outside the main plane of the links, known as Out of Plane Bending (OPB) was considered. The loads increase the resulting friction allocated in the contact between the links, making it behave like a bezel, so transverse forces result in bending out of the plane. The loadings come due to the platforms operating under various factors of nature, such as variations in waves and sea currents, in addition to the operating conditions of the platform. Thus, FPSO ships, designed to last more than twenty years, recorded cases of failure in the anchoring system in less than two years. The material used in the model of the links was offshore steel belonging to grade R4. The simulations were carried out with winding angles of 60°, with loads in the range of 200 and 400 ton being applied. With the result of this analysis, it is possible to validate the hotspots in the links of the moorings, identifying the influence of the winding angle. Thus, it is possible to validate the equations that describe the behavior of the mooring-fairlead set taking in consideration the transverse and axial loads. Finally, the fatigue life of the links was calculated using the Smith-Watson-Toper (SWT) fatigue criterion, considering a loading with variable amplitude.

Keywords: Mooring-fairlead, hotspots, Out-of-plane Bending, steel grade R4, SWT.

1 Introduction

Due to the fact that much of the exploration and extraction of oil and gas takes place on offshore platforms, demands for new mooring system technologies have arisen for these platforms [7,21]. According to Mamiya et al. [12], one of these demands was a technology of devices for the fixation of the platforms on the ocean floor. Due to the discovery of oil in deep waters (depth greater than a thousand meters), floating platforms have gained notoriety in the offshore scenario. The Floating, Production, Storage and Offloading (FPSO) are fixed through an anchoring system. Such lines are composed of stretches with polymeric materials or steel cable, where the moorings (chains) and an anchor are connected [2,18]. According to Liu et al. [11], François [5] and Lian et al. [10], the combination of these materials occurs in order to reduce the weight of the entire system, given the great depth that the wells are located.

The anchor lines are designed to have a service life of more than twenty years of operation without the intervention or replacement of components. However, premature failures occurred in less than two years of operation, such failures were reported in the early 2000s. Although the lines were designed following the guidance of the American Petroleum Institute (API), failures occurred in relatively short periods when compared to the expected design time [9].

As reported by Vargas and Jean [19], due to the frictional force in the contact of the links being accentuated, there is an impediment of their rolling with each other during operations on the platform. Consequently, the bending resistance increases, resulting in cyclic bending efforts, which in a short period of time, promote the initiation and propagation of fatigue cracks in the chain links. According to Jean et al. [8], the tensions caused by the out-of-plane bending mechanism (OPB) are detrimental to the fatigue life of the chains.

The material applied in the oil and gas industry is classified as Grade R offshore material, ranging from R3 to R5 [3,13]. According to Silva [18], in the initial stretch, the mooring lines are composed of a sequence of high

mechanical resistance steel links that start inside the FPSO platforms and pass through a guide device, called a fairlead towards the sea. The junction of the chains with the fairlead generates a system called mooring-fairlead. Such a system has a crown that allows the rotation of the links of the chains, one in relation to the other, adjusting the platform regarding the movement of the sea. As reported by Neves [14], structural failures usually occur in the moorings located at the top of the anchorage sections exactly where there is a combination between moorings and fairleads.

2 Theoretical background

2.1 Material properties

Table 1 presents the monotonic mechanical properties of grade R4 offshore steel. The properties were obtained through a conventional tensile test and an optimized process of parametric identification. All calibration and characterization of the material was performed by Neves [14].

Table 1. Monotonic properties offshore steel grade R4 [14].

Monotonic Properties	Symbol	Values
Young's Modulus	$\boldsymbol{E}$ [GPa]	207.4
Poisson's ratio	$\boldsymbol{\nu}$	0.3
Initial yield stress	$\boldsymbol{\sigma_{y0}}$ [MPa]	836.6
Ultimate stress	$\boldsymbol{\sigma_u}$ [MPa]	888.7
Rupture stress	$\boldsymbol{\sigma_r}$ [MPa]	475
Percentual elongation	$\boldsymbol{AL}$	24.2 %
Reduction of area	$\boldsymbol{RA}$	0.693

For cyclic characterization, the kinematic hardening curve of steel was defined using the Armstrong-Frederick [6], along with the Ramberg-Osgood [15] formulation presented in Table 2.

Table 2. Cyclic properties of grade R4 offshore steel [14]

Cyclic Properties	Symbol	Values
Cyclic strength coefficient	$\boldsymbol{K'}$[MPa]	1730.2
Cyclic stain hardening exponent	$\boldsymbol{n'}$	0.1185
Kinematic hardening modulus	$\boldsymbol{H^K}$[MPa]	52151.5
Saturation coefficient	$\boldsymbol{b}$	181.3
Cyclic yield stress	$\boldsymbol{\sigma_y^*}$[MPa]	720.3
Coefficient of fatigue resistance	$\boldsymbol{\sigma_f'}$	6916.5
Exponent of fatigue resistance	$\boldsymbol{b'}$	- 0.237

2.2 Manufacture of chains

To be characterized as offshore material, the moorings have to comply with some standards. In view of this, two fundamental parameters are established. The first test is to obtain the Minimum Break Load (MBL), whose definition is given through laboratory tests applying a monotonic load until a link breaks. The minimum applied load for breaking is assumed as the MBL of the current, which is an important design parameter. Another important parameter is the proof load, defined as a percentage of the MBL. According to the standard, this proof load can vary between 50% and 75% of the MBL [3,8,20]. With the application of this proof load, if the chain does not break, it is ready for real operations. Such a process contributes to the certification of the resistance of the systems, but, on the other hand, it generates excessive plastic deformations in the contacts of the links that considerably increase the friction force, in this way, this contributes for the links to behave like crimps [4,17,21].

For this work, the adopted MBL is 1200 tons and the proof load is 900 tons. For oscillatory loads, the minimum load is 200 tons (1/6 MBL) and the maximum 400 tons (1/3 MBL). The minimum load represents the

chain's own weight.

3 Analytical and numerical analysis

3.1 Analytical study of the equilibrium of the system

The mathematical development consists of deducing an analytical equation to determine the normal stress in the critical regions of the links of interest, since the occurrences of premature failures are evidenced in this region of the system. Figure 1 shows the free-body diagram of the mooring-fairlead set. From the diagram, it is possible to define the components of axial and transverse forces, causing normal stress in the chain link hotspot. The angle θ is defined as the angle of fairlead operation or winding [12], ranging between 17° and 60°, of according to the mooring-fairlead system designed by the company AmClyde. The angle α is the fairlead rotation angle, which varies according to the amplitude of the load applied.

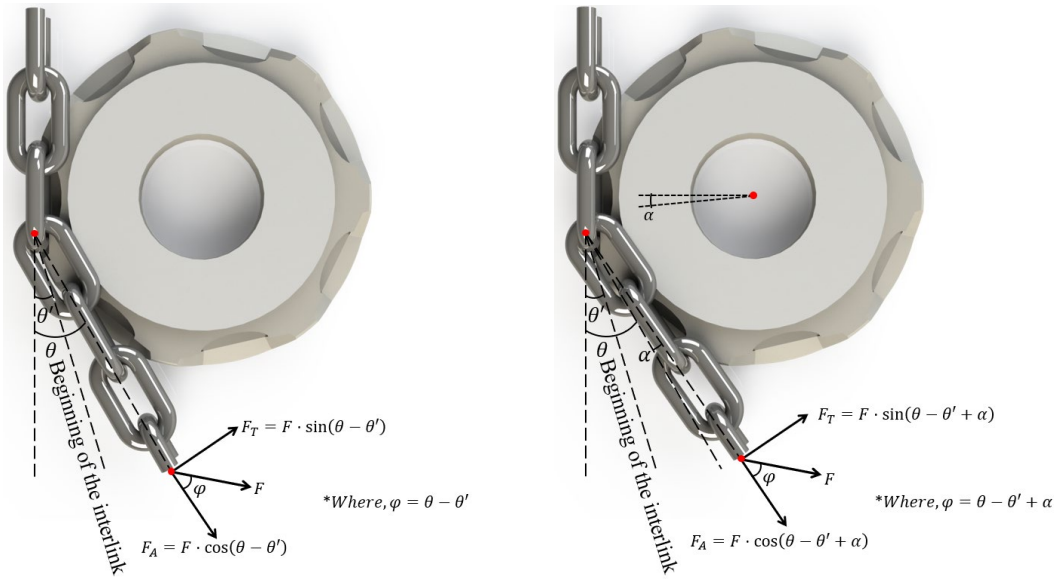

Figure 1. a) Mooring-fairlead set with application of the minimum load $(\theta - \theta')$. b) Mooring-fairlead set with maximum load application $(\theta - \theta' + \alpha)$.

Through the analysis of the efforts present in the mooring-fairlead, it is possible to define equations for the minimum and maximum loading. The equations are written with two plots, one part of the stress is due to the contribution of the axial force (σ_A) and another due to the contribution of the out-of-plane bending (σ_{OPB}). The equation Eq.(1) describes the requests at the minimum load and the Eq. (2) describes for maximum loading.

$$\sigma_{mín} = C_a \frac{2F_{mín}\cos(\theta - \theta')}{\pi d^2} + C_{OPB}\frac{16F_{mín}L_i \sin(\theta - \theta')}{\pi d^3} \tag{1}$$

$$\sigma_{máx} = C_a \frac{2F_{máx}\cos(\theta - \theta' + \alpha)}{\pi d^2} + C_{OPB}\frac{16F_{máx}L_i \sin(\theta - \theta' + \alpha)}{\pi d^3} \tag{2}$$

Where, θ' is defined as the interlink angle, this angle indicates when the locking starts, the locking of the links is directly related to the out-of-plane bending. The cross-sectional area of the link is defined as, $A = \pi d^2/4$ and the inertia as, $I = \pi d^4/64$. Being d the diameter of the link, in which the value of 120 mm was adopted. "L_0" is the distance from link locking to the load application point. C_a and C_{OPB} are constants that are related to the link geometry.

3.2 Analysis on finite elements method

In Figure 2 a) we have the mooring-fairlead set assembled, with the respective components. As the stress analysis will only be on the links, the fairlead crown was modeled as a rigid body. The spring elements are responsible for simulating all the stiffness of the links that are present inside the FPSO platform. The links named as of interest are the links susceptible to out-of-plane bending, as they have a higher probability of premature failure. Those represented in red, in Figure 2 a), such as links "C" and "E". The inner part of the links (part where the face of the link is in contact with the fairlead, Figure 2 a)) is where the incidence of hotspots occurs.

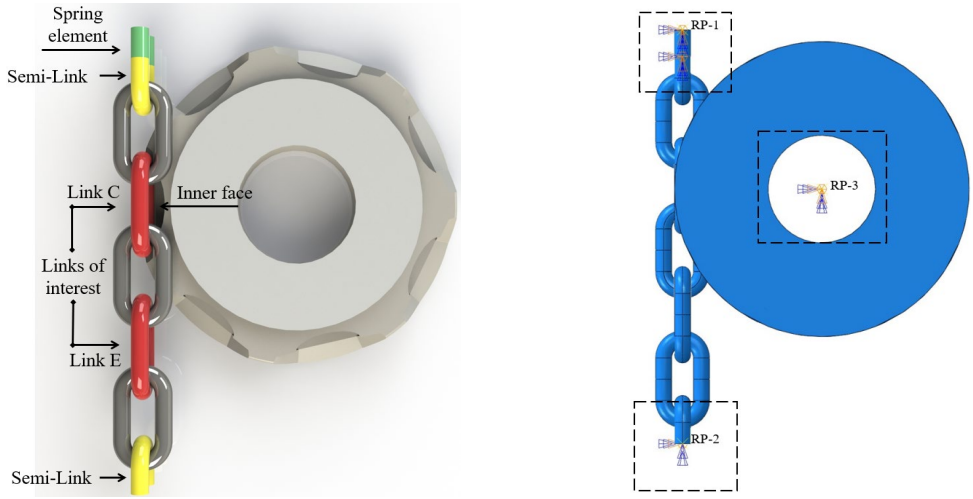

Figure 2. a) Assembly of the real scale mooring-fairlead. b) Mooring-fairlead assembly in the ABAQUS CAE©.

At first, eight Steps were defined for the simulation. Two are defined as static analysis and the rest as implicit dynamic analysis.

Steps are defined as CP, S-CP, CT1-1-1, CT2-1, CT1-2, C2-2, CT1-3 and CT2-3. The CP and S-CP are the static Steps, where the first proof load is applied and the second one is removed. Steps from CT1-1-1 to CT2-3 are defined as dynamic, where there is load variation. For the application of loading and boundary conditions, three "reference points" (RP-1, RP-2 and RP-3) were used, as shown in Figure 2 b). For this study, six boundary conditions were used. These settings apply across Steps and are defined as BC-1, BC-2, BC-3, BC-4, BC-5, and BC-6. The conditions are defined below.

• BC-1 – Condition of type Displacement/Rotation, applied on the faces of the spring element. Constraint of displacements and rotations in X, Y and Z directions. Boundary condition applied in Steps CP and S-CP.

• BC-2 – Displacement/Rotation type condition applied to "RP-2", displacement only in "Y" direction, displacements in X and Z direction and rotations in constrained X, Y and Z directions. Boundary condition applied in Steps CP and S-CP.

• BC-3 – Displacement/Rotation type condition, applied in "RP-3". For static steps, restriction of displacements and rotations in the X, Y and Z directions. For dynamic steps, restriction of displacements in the X, Y and Z directions and rotations in the X and Y directions.

• BC-4 – Displacement/Rotation type condition applied to "RP-1". Constraint of displacements and rotations in X, Y and Z directions. Boundary condition applied in dynamic Steps.

• BC-5 – Condition of type Displacement/Rotation, applied on the faces of the spring element. Constraint of displacements in the X and Z directions and rotations in the X, Y and Z directions. Boundary condition applied in dynamic Steps.

• BC-6 – Symmetry/Antisymmetry/Encastre type condition applied to "RP-2", restriction of displacement in the Z direction and rotations in the X and Y directions. Boundary condition applied to the dynamic Steps.

For each component of the set, the finite element mesh was modeled in a different way. The fairlead is

discretized with quadrilateral and triangular finite elements, both linear elements and with reduced integration. The deformation cylinder, independent solids, semi-links and links are discretized with linear hexahedral finite elements with reduced integration. The total number of nodes in the assembly is 209739 and the number of elements is 178617.

The type of contact applied was surface-to-surface and the slip formulation considered was of the large displacement type and the discretization method is of the surface-to-surface type. The contact properties considered were normal and tangential. For the normal contact, "Hard" - Contact was used for the activation pressure and for the contact imposition method, it was considered as "Default" (Lagrangian Formulation). As for the tangential contact, the friction formulation was of the "Penalty" type and the coefficient of friction adopted was 0.7 [12]. For all numerical analysis, the ABAQUS® software version 2017 was used.

4 Results and discussion

4.1 Analysis of stresses in the links of interest

The minimum and maximum loads are composed of axial stress and out-of-plane moment contributions. In Table 3 we have the values calculated analytically. The displayed values refer to the stresses of the links of interest, links "C" and "E". For this analysis, a winding angle equal to 60° (θ = 60°) was considered. In addition, three interlink angles were considered. In the first consideration, the interlink angle is equal to the winding angle ($\theta' = \theta$). In the second consideration, the interlink angle equals zero ($\theta' = 0$), and in the third consideration, the difference between the winding and interlink angle is 3° ($\theta - \theta' \cong 3$).

Table 3 Minimum and maximum normal stresses at hotspot, using the 60° winding angle.

$\theta = 60°$		Minimum load [200 tons]			Maximum load [400 tons]		
$\alpha = 1.9386$		σ_A	σ_M	$\sigma_{mín}$	σ_A	σ_M	$\sigma_{máx}$
Link C	$\theta' = \theta$	260.00	–	**260.00**	519.70	228.21	**747.91**
	$\theta' = 0$	130.00	2921.09	**3051.09**	244.62	5952.95	**6197.56**
	$\theta - \theta' \cong 3°$	259.64	176.53	**436.17**	518.07	580.75	**1098.82**
Link E	$\theta' = \theta$	260.00	–	**260.00**	519.70	163.01	**682.71**
	$\theta' = 0$	130.00	2086.49	**2216.49**	244.62	4252.10	**4496.72**
	$\theta - \theta' \cong 3°$	259.64	126.09	**385.74**	518.07	414.82	**932.89**

Figure 3 demonstrates the results after the simulation in the inner portion of the links of interest, where there is an incidence of hotspots. The hotspot can be defined as points of maximum stress, where it has the highest probability of crack initiation [16]. In Figure 3, the results are found considering the minimum and maximum loading, for both links of interest analyzed in the study.

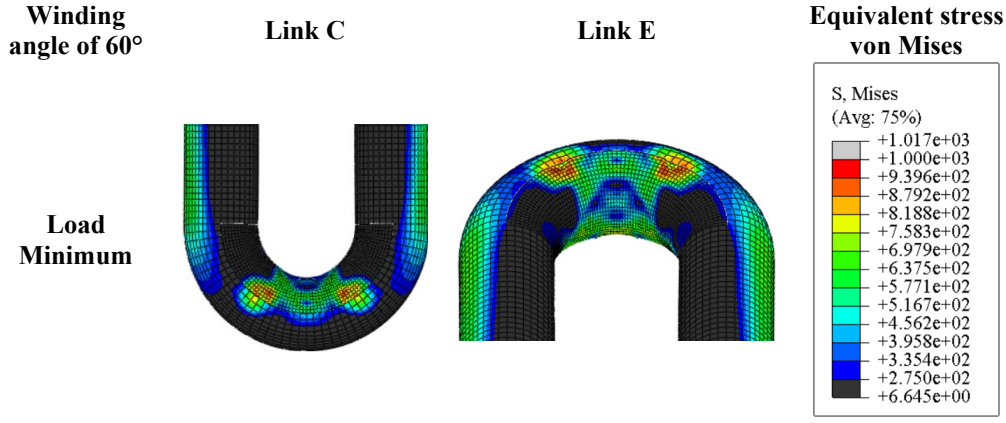

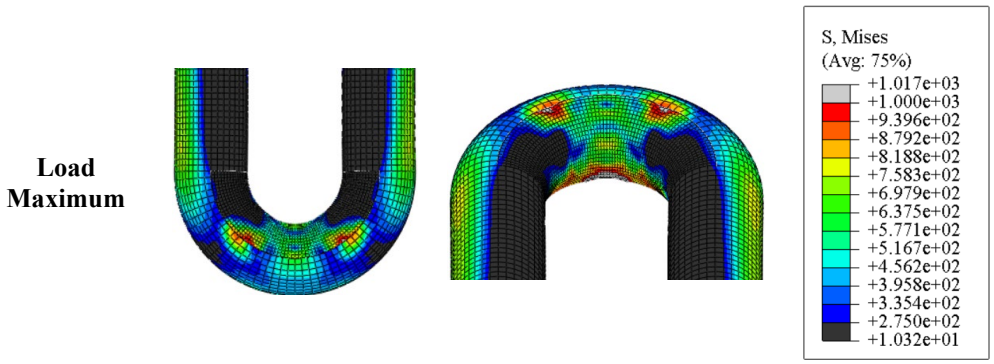

Figure 3. Contours of equivalent stress on the inside of the links of interest under minimal and maximal loading.

According to Table 3 and the results obtained through the simulations, Figure 3, it is possible to notice that the interlink angle cannot be equal to zero nor equal to the winding angle. The analytical results that are closest to the numerical results are when the difference between the winding and interlink angle is equal to 3°. In a way, the interlink angle is a variable of great importance, as it indicates the beginning of the links locking, generating out-of-plane bending, contributing to premature failure. It is notorious that the consideration made of the equality between the interlink angle and the winding angle, which generates the stresses found in Table 3, has only contribution from the axial load. Already, considering the interlink angle equal to zero, it is observed that the stress contribution due to transverse loading increases considerably. Thus, it is concluded that the smaller the interlink angle, the greater the out-of-plane stresses. Comparing the analytical and numerical results, for the minimum load, the analytical values for both the "C" and "E" link are smaller than the values found in the numerical analysis. As for the maximum loading values, the analytical and numerical values are very close. Figure 3 shows that both links "C" and "E" have very evident accentuation of hotspots.

4.2 Fatigue life of the links of interest under loading with variable amplitude

For the analysis of the fatigue life of the links of interest under loading with variable amplitude, two loading cases were proposed, both with variable amplitude. Thus, the first case has two ranges of amplitudes, where the first range goes from 200 to 280 tons and the second from 200 to 230 tons. In the second case, there are four ranges of amplitudes. The first range considers a load of 200 to 220 tons, the second 200 to 290 tons, the third 200 to 250 and the fourth 200 to 310 tons. Figure 4 demonstrates the loading histories used in the study.

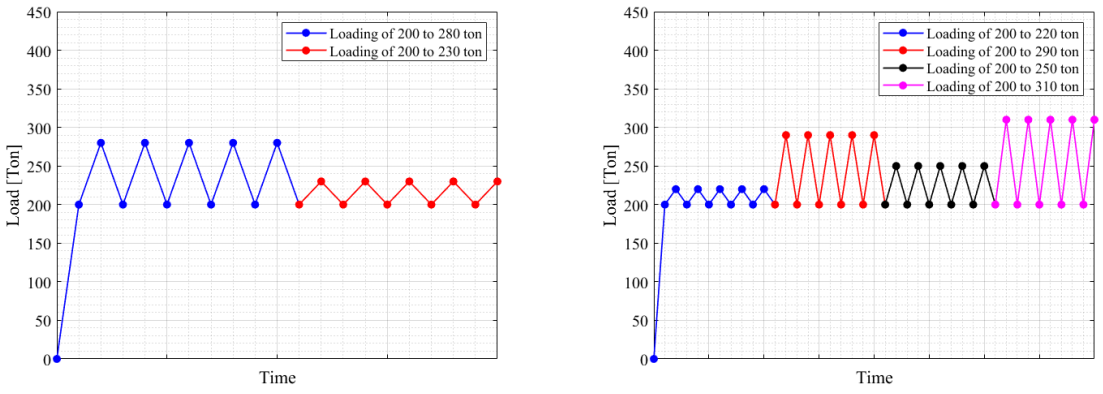

a) b)

Figure 4. Loads under variable amplitude. a) 200 to 280 tons and 200 and 230 tons. b) 200 to 220 tons, 200 to 290 tons, 200 to 250 tons and 200 and 310 tons.

With equations (1) and (2) it is possible to calculate the minimum and maximum stresses at the hotspot. For

the calculations, three winding angles were taken into account, being 17°, 38.50° and 60°. For both angles, the difference between the winding and interlink angle of 3° was considered. To calculate the number of N_f cycles, the fatigue life criterion SWT and the relationship proposed by Basquim [1] were used. Thus, with equation (3) it is possible to determine the number of cycles. Where σ_a is the stress amplitude and σ_f' and b' represents the coefficient and exponent of fatigue resistance of the offshore material grade R4 (Table 2). From the number of cycles, it is possible to determine the lifetime using a frequency of 0.1 Hz for each cycle [12].

$$N_f = \left(\frac{\sqrt{\sigma_a \sigma_{máx}}}{\sigma_f'}\right)^{\frac{1}{b'}} \tag{3}$$

For the first case of proposed loading, in Figure 5 a) it is possible to observe that, when the chains are subjected only to loading without the OPB effect, they have lives close to 63 years of operation, for both links of interest and winding angles analyzed. When you have the incidence of the OPB effect, there is a reduction in lives. Despite the lives with OPB effect being greater than in one year of operation, the "C" link has a shorter life when compared to the "E" link. The variation of the winding angles did not have a great influence on the results of the lifetimes, as the results are similar.

For the second case, in Figure 5 b), it is possible to observe that, when the chains are subjected only to loading without the OPB effect, they have lives close to 174 years of operation, for both links of interest and for all angles winding analyzed. Already, with the incidence of the OPB effect, there is a reduction in lives. For a winding angle of 17°, the "C" link has a life of about 11 years and the "E" link has a life close to 20 years of operation. For winding angles of 38, 50° and 60°, the "C" link has an operational life of about 10 years and the "E" link 19 years. In a way, this shows us that the "C" link suffers more in relation to the incidence of OPB, as well as in the previous cases. Winding angles of values of 38,50° and 60° with loading under the effect of OPB have shorter lives when compared to the angle of 17°. Here, in this case, there is a small influence of the winding angle on the life of the chains.

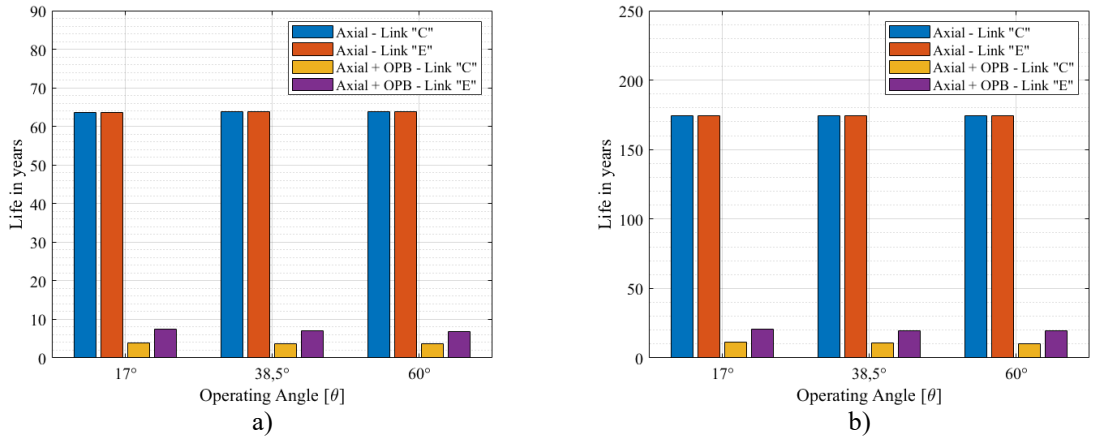

Figure 5. Life in years of chains for loading with variable amplitude. a) First case. a) Second case.

5 Conclusions

With the results obtained after the simulation and the calculations made through the equations, it is possible to analyze the behavior of the links in the mooring-fairlead set. As previously reported, anchorage systems exhibit premature failure within short operating times, and one of the predominant factors for failure is out-of-plane bending.

Life analysis was with variable amplitude loading. Thus, two loading cases for variable amplitude were proposed. As expected, the greater the loading amplitude, the shorter the life. Another factor that contributes to a shorter life is the OPB effect, an effect disregarded by the API standard.

The results observed for loading with variable amplitude, demonstrate that the OPB effect reduces the life of the links, this for the two cases of loads analyzed. The results also showed that the "C" link suffers more from the

OPB effect, when compared to the "E" link.

The results of the lives obtained with the analyzed winding angles are very close. Thus, as a suggestion for future work, it is recommended to define the locking moment of the link (θ'), so that it is possible to refine the analysis of out-of-plane bending and, consequently, the analysis of lives.

Acknowledgements. The authors thank the University of Brasilia for their support, CAPES and CNPQ.

Authorship statement. The authors hereby confirm that they are the sole liable persons responsible for the authorship of this work, and that all material that has been herein included as part of the present paper is either the property (and authorship) of the authors, or has the permission of the owners to be included here.

References

[1] O.H. Basquim, The exponential law of endurance tests, American Society for Testing Materials. 10 (1910) 625–630.
[2] K. Berthelsen, Out of plane bending of mooring chains - finite element analysis of a 7-link model, PhD Thesis, Norwegian University of Science and Tecnology, 2017.
[3] F.A. Canut, A.M.P. Simões, L. Reis, M. Freitas, I.N. Bastos, F.C. Castro, E.N. Mamiya, Monitoring of corrosion-fatigue degradation of grade R4 steel using an electrochemical-mechanical combined approach, Fatigue Fract Eng Mater Struct. 42 (2019) 2509–2519.
[4] J. Choung, J. Lee, Y. Hun Kim, Out-of-plane bending stiffnesses in offshore mooring chain links based on conventional and advanced numerical simulation techniques, Journal of Ocean Engineering and Technology. 32 (2018) 297–309.
[5] M. François, P. Davies, F. Grosjean, F. Legerstee, Modelling fiber rope load-elongation properties-polyester and other fibers, in: Offshore Technology Conference - OTC, Houston, Texas, USA, 2010.
[6] C.O. Frederick, P.J. Armstrong, A mathematical representation of the multiaxial Bauschinger effect, Materials at High Temperatures. 24 (1966) 1–26.
[7] I.A. Ja'e, M. Osman Ahmed Ali, A. Yenduri, Z. Nizamani, A. Nakayama, Optimisation of mooring line parameters for offshore floating structures: A review paper, Ocean Engineering. 247 (2022).
[8] P. Jean, K. Goessens, D. L'Hostis, Failure of Chains by Bending on Deepwater Mooring Systems, in: Offshore Technology Conference, Houston, Texas, USA, 2005: pp. 2–5.
[9] Y. Kim, M.S. Kim, M.J. Park, Fatigue analysis on the mooring chain of a spread moored FPSO considering the OPB and IPB, International Journal of Naval Architecture and Ocean Engineering. 11 (2019) 178–201.
[10] Y. Lian, B. Zhang, J. Zheng, H. Liu, G. Ma, S.C. Yim, Y. Zhao, An upper and lower bound method for evaluating residual strengths of polyester mooring ropes with artificial damage, Ocean Engineering. 262 (2022).
[11] H. Liu, W. Huang, Y. Lian, L. Li, An experimental investigation on nonlinear behaviors of synthetic fiber ropes for deepwater moorings under cyclic loading, Applied Ocean Research. 45 (2014) 22–32.
[12] E.N. Mamiya, F.C. de Castro, L. Malcher, T. de C.R. Doca, P.V. Muterlle, L.F.G. dos Reis, M.J.M. de Freitas, V.I.M.N. Infante, A.M.R. Ribeiro, Relatório Técnico FINAL - Durabilidade de componentes de Sistemas de Amarração para uso em águas profundas: experimentação e modelagem DSAm, Brasília, 2019.
[13] I. Martinez Perez, A. Constantinescu, P. Bastid, Y.H. Zhang, V. Venugopal, Computational fatigue assessment of mooring chains under tension loading, Eng Fail Anal. 106 (2019).
[14] R.S. Neves, Uma extensão do modelo de Gurson para análise de fadiga seguindo uma metodologia incremental, Tese de Doutorado, Universidade de Brasília, 2020.
[15] W. Ramberg, W.R. Osgood, Description of stress-strain curves by three parameters, in: Technical Report N° 092 - National Advisory Committee for Aeronautics, Washington, 1943.
[16] L. Rampi, F. Dewi, S. Offshore, P. Vargas, Chain out of plane bending (OPB) joint industry project (JIP) summary and main results, in: Offshore Technology Conference, Houston, Texas, USA, 2015: pp. 4–7.
[17] L. Rampi, P. Vargas, Fatigue testing of out-of-plane bending mechanism of chain links, in: Proceedings of the International Conference on Offshore Mechanics and Arctic Engineering - OMAE, Hamburg, Germany, 2006.
[18] M.Z. e Silva, Estudo da influência do desgaste na falha prematura de componentes de linhas de ancoragem, Dissertação de Mestrado, Universidade de Brasília, 2016.
[19] P. Vargas, P. Jean, FEA of out-of-plane fatigue mechanism of chain links, in: Proceedings of the International Conference on Offshore Mechanics and Arctic Engineering - OMAE, Halkidiki, Greece, 2005: pp. 173–182.
[20] E.P. Zarandi, B.H. Skallerud, Cyclic behavior and strain energy-based fatigue damage analysis of mooring chains high strength steel, Marine Structures. 70 (2020) 102703.
[21] E.P. Zarandi, B.H. Skallerud, Experimental and numerical study of mooring chain residual stresses and implications for fatigue life, Int J Fatigue. 135 (2020) 105530.